



Transition metal M(II) complexes with isonicotinic acid 2-(9-anthrylmethylene)-hydrazide

MARIANA LOREDANA DIANU^{1*}, ANGELA KRIZA¹, NICOLAE STANICA²
and ADINA MAGDALENA MUSUC²

¹University of Bucharest, Faculty of Chemistry, Department of Inorganic Chemistry, 23 Dumbrava Rosie St., 020464 Bucharest and ²Romanian Academy, "Ilie Murgulescu" Institute of Physical Chemistry, 202 Spl. Independentei, P.O. Box 12–194, 060021 Bucharest, Romania

(Received 23 November 2009, revised 6 April 2010)

Abstract: New complexes of isonicotinic acid 2-(9-anthrylmethylene)-hydrazide with Cu(II), Co(II) and Ni(II) have been prepared and characterized by analytical and physico-chemical techniques, such as elemental and thermal analyses, magnetic susceptibility and conductivity measurements, and electronic, EPR and IR spectral studies. The infrared spectral studies revealed the bidentate or monodentate nature of the Schiff base in the complexes; the pyridine nitrogen does not participate in the coordination. A tetrahedral geometry is suggested for the nitrate complexes and an octahedral geometry for the others. Thermal studies support the chemical formulation of these complexes.

Keywords: IR spectra; isonicotinoylhydrazone; Schiff base; transition metal complexes; thermal analysis.

INTRODUCTION

It is generally known that hydrazones have significant antimicrobial, anti-convulsant, analgesic, anti-inflammatory and antitumoral activities.^{1–6} The remarkable biological activity of acid hydrazides R–CO–NH–NH₂, their corresponding arylhydrazones R–CO–NH–N=CH–R', and the dependence of their activity on the mode of chelating with transition metal ions have been of significant importance in the past.^{7–10} Thermal analysis techniques (DTA, TG, DSC) play an important role in the study of the structure of metal complexes.^{11–16}

As a continuation of our interest in the coordination behavior of Schiff bases with isonicotinoylhydrazones,¹⁷ the synthesis and characterization of a series of copper(II), cobalt(II) and nickel(II) complexes with the isonicotinic acid 2-(9-anthrylmethylene)-hydrazide ligand are reported herein.

*Corresponding author. E-mail: maridianu@yahoo.com
doi: 10.2298/JSC091113121D

EXPERIMENTAL

Materials

All chemicals were of pure analytical grade and were purchased from Sigma-Aldrich and Fluka.

Methods and apparatus

The Schiff base ligand was prepared by a known method.¹⁸ The metal(II) contents were determined by literature methods.¹⁹ The carbon, hydrogen and nitrogen contents were determined using CHNS-O elemental combustion analysis with a Costech elemental analyzer, model ECS 4010. The melting temperatures of the complexes were directly measured with SMPI Melting Point apparatus. The molar conductance of the complexes was measured at a concentration of 1.0×10^{-3} M in DMF at room temperature using a Consort type C-533 conductivity instrument. The IR spectra were recorded between 4000–400 cm⁻¹ in KBr pellets with a Bio-Rad FTS-135 instrument. The reflectance spectra of the complexes were recorded on a Jasco V-670 spectrophotometer. The EPR spectra for the copper(II) complexes were recorded using a Jeol JES-FA 100 X-band frequency spectrometer. Measurements of the magnetic susceptibility were realized at room temperature using the Faraday method and were corrected for diamagnetism.

The thermal experiments were performed on a Mettler Toledo TGA/SDTA 851^e thermal analyzer, within the temperature range 25–1000 °C, and a Mettler Toledo DSC 853^e differential scanning calorimeter, within the temperature range 25–600 °C. The TG curves were recorded under a dynamic nitrogen atmosphere at a flow rate of 50 mL min⁻¹ and at a heating rate of 10 K min⁻¹. The DSC curves were obtained under a dynamic nitrogen atmosphere at 80 mL min⁻¹ flow rate and the same heating rate. The samples were held in aluminum crucibles for the DSC experiments and Al₂O₃ crucibles for the TG/SDTA experiments, with a pinhole in the lid, for both methods, to prevent pressure build up due to gaseous products. The sample mass was between 0.8 and 3 mg for both methods. At the end of the heating process for the DSC experiments, the mass of the remaining sample represented approximately 30–40 % of the initial value for all the studied complexes. The TG and DSC curves were used to characterize the variation of mass and also thermal changes during the linear heating.

Synthesis of complexes

A methanolic solution (10 mL) of isonicotinoylhydrazide (1.0×10^{-3} M) and a methanolic solution (20 mL) of 9-anthraldehyde (1.0×10^{-3} M) were mixed with constant stirring at 50 °C for 30 min. The preparation of the complexes was performed by mixing methanolic solutions (1.0×10^{-3} M, 20 mL) of metal (Cu(II), Co(II) and Ni(II)) salts (nitrate, acetate and perchlorate) to a cold methanolic solution of the ligand. The reaction mixture was stirred under reflux for 3 h. The obtained precipitates were filtered, washed with methanol and dried under vacuum on anhydrous CaCl₂.

RESULTS AND DISCUSSION

The synthesized complexes have the general formulae ML₂X₂·xH₂O, where M = Cu(II), Co(II) or Ni(II), L = Schiff base (Fig. 1) and X = NO₃⁻, ClO₄⁻ or CH₃COO⁻.

The complexes were characterized based on elemental analyses, magnetic susceptibility and electronic conductivity measurements, IR, UV-Vis-NIR and EPR spectroscopy and thermal studies. The M(II) complexes were colored pow-



ders with high melting points. They were soluble in acetone, DMF and DMSO and insoluble in methanol, ethanol, CHCl_3 , CH_2Cl_2 and CCl_4 .

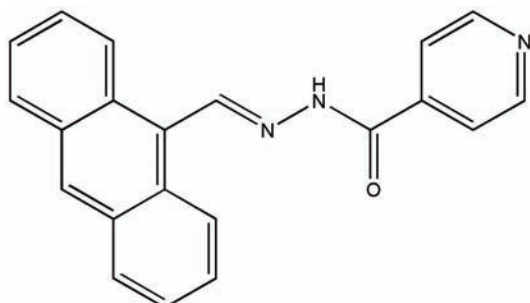


Fig. 1. Structural formula of isonicotinic acid 2-(9-anthrylmethylene)-hydrazide (L).

The analytical and physical data (color, melting point and molar conductivity in DMF (1.0×10^{-3} M, at room temperature)) of the complexes are given in Table I. The molar conductivity values show that the nitrate and perchlorate complexes were 1:2 electrolytes and the acetate complexes were non-electrolytes.²⁰

TABLE I. Analytical and physical data of the complexes

Compound	Color	Found (Calcd.), %				M.p. °C	A_M^a $\Omega^{-1} \text{cm}^2 \text{mol}^{-1}$
		C	H	N	M		
$[\text{CuL}_2(\text{H}_2\text{O})_2](\text{NO}_3)_2 \cdot 2\text{H}_2\text{O}$	Green (I)	56.03 (55.41)	4.11 (4.21)	12.96 (12.31)	6.55 (6.98)	>320	154
$[\text{NiL}_2(\text{H}_2\text{O})_2](\text{NO}_3)_2 \cdot 4\text{H}_2\text{O}$	Yellowish green (II)	54.21 (53.57)	4.26 (4.49)	12.54 (11.90)	5.97 (6.23)	>320	148
$[\text{CuL}_2(\text{H}_2\text{O})_2](\text{ClO}_4)_2$	Reddish (III)	53.88 (53.14)	3.34 (3.61)	9.16 (8.85)	6.23 (6.69)	285 ^a	137
$[\text{CoL}_2(\text{H}_2\text{O})_2](\text{ClO}_4)_2$	Brick-red- -colored (IV)	54.12 (53.40)	3.28 (3.63)	9.21 (8.89)	5.98 (6.24)	260 ^a	175
$[\text{NiL}_2(\text{H}_2\text{O})_2](\text{ClO}_4)_2$	Orange (V)	53.69 (53.41)	3.76 (3.63)	9.26 (8.90)	6.32 (6.21)	250 ^a	143
$[\text{CuL}_2(\text{CH}_3\text{COO})_2]$	Khaki (VI)	66.82 (66.37)	4.12 (4.36)	10.32 (10.09)	7.24 (7.63)	>320	3.4
$[\text{CoL}_2(\text{CH}_3\text{COO})_2] \cdot 2\text{H}_2\text{O}$	Brown- reddish (VII)	64.42 (63.96)	4.33 (4.67)	10.16 (9.73)	6.63 (6.82)	>320	5.2
$[\text{NiL}_2(\text{CH}_3\text{COO})_2]$	Green- khaki (VIII)	68.09 (66.76)	4.55 (4.38)	10.48 (10.16)	7.24 (7.09)	>320	4.5

^aWith decomposition

Infrared spectra

The IR spectra of the Schiff base (L) and its metal complexes were recorded between 4000–400 cm^{-1} and the obtained data are summarized in Table II with some assignments of the important characteristic bands.

TABLE II. The characteristic IR bands (cm^{-1}) of the ligand and the complexes ($\text{X}^- = \text{NO}_3^-$, ClO_4^- , CH_3COO^-)

Compound	$\nu(\text{O}-\text{H})$	$\nu(\text{C}=\text{O})$ Amide I	$\nu(\text{C}=\text{N})$ Azomethine	$\delta(\text{N}-\text{H})$ Amide II	ν_{X}^-	$\rho_r(\text{H}_2\text{O})$
Ligand (L)	—	1654	1597	1520	—	—
$[\text{CuL}_2(\text{H}_2\text{O})_2](\text{NO}_3)_2 \cdot 2\text{H}_2\text{O}$ (I)	3421	1652	1558	1507	1384	849
$[\text{NiL}_2(\text{H}_2\text{O})_2](\text{NO}_3)_2 \cdot 4\text{H}_2\text{O}$ (II)	3430	1653	1550	1510	1384	849
$[\text{CuL}_2(\text{H}_2\text{O})_2](\text{ClO}_4)_2$ (III)	3430	1637	1569	1510	1106, ν_3 623, ν_4	850
$[\text{CoL}_2(\text{H}_2\text{O})_2](\text{ClO}_4)_2$ (IV)	3367	1635	1551	1521	1088, ν_3 625, ν_4	841
$[\text{NiL}_2(\text{H}_2\text{O})_2](\text{ClO}_4)_2$ (V)	3420	1661	1564	1519	1108, ν_3 625, ν_4	845
$[\text{CuL}_2(\text{CH}_3\text{COO})_2]$ (VI)	—	1653	1557	1520	1570, ν_{asym} 1493,	—
$[\text{CoL}_2(\text{CH}_3\text{COO})_2] \cdot 2\text{H}_2\text{O}$ (VII)	3390	1652	1547	1521	1571, ν_{asym} 1498,	—
$[\text{NiL}_2(\text{CH}_3\text{COO})_2]$ (VIII)	—	1653	1550	1522	1572, ν_{asym} 1450, ν_{sym}	—

The IR spectra of the complexes **I–V** and **VII** showed a broad band at 3400 cm^{-1} that can be assigned to the $\nu_a(\text{OH})$ and $\nu_s(\text{OH})$ vibration modes from water molecules.²¹ The presence of coordinated water was confirmed by the medium strength bands at 840–850 cm^{-1} , characteristic of $\rho_r(\text{H}_2\text{O})$ frequencies. These bands were not observed in the spectra of the complexes **VI** and **VIII**, indicating the absence of coordinated water molecules.

The IR spectrum of the ligand exhibits two medium bands at 3196 and 3047 cm^{-1} , which can be ascribed to the asymmetric and symmetric vibrational frequencies of the NH amide group, respectively. The band at 1520 cm^{-1} was assigned to $\delta(\text{N}-\text{H})$ of amide II. This band appeared in the spectra of the ligand and complexes at the same position, confirming that the nitrogen atom of the NH moiety does not participate in the coordination. The observed minor shift to lower frequencies of $\delta(\text{N}-\text{H})$ (amide II) for some complexes (**I–III**) may be due to the presence of the amide group in a chelate system rather than in the open system of the ligand.¹⁴

The band at 1654 cm^{-1} , attributable to the $\nu(\text{C}=\text{O})$ stretching vibration of the Schiff base ligand²² is shifted to another region in the complexes **III–V**, indicating coordination of the carbonyl oxygen to the metal ions. The presence of bands at 520–550 cm^{-1} in the IR spectra of complexes **III–V** is due to M–O stretching vibrations.²³



The azomethine band at 1597 cm^{-1} was shifted to lower frequencies in the spectra of all the complexes, confirming the participation of the azomethine nitrogen atom in the coordination of the metal ions. In the IR spectra of these complexes, the new bands which appear in the $460\text{--}420\text{ cm}^{-1}$ region are assigned to the $\nu(\text{M-N})$ vibration.¹⁷

The band at 1623 cm^{-1} , assigned to the vibration of the pyridine ring, remains at the same position in the spectra of the ligand and complexes, confirming that the nitrogen of pyridine group does not participate in the coordination.

The strong sharp band observed at 1384 cm^{-1} in the complexes **I** and **II** can be assigned to uncoordinated nitrate ion.²⁴ In the IR spectra of complexes **III**–**V**, the presence of strong ν_3 at about 1100 cm^{-1} and medium ν_4 at 625 cm^{-1} bands indicates that the T_d symmetry of the perchlorate anion is maintained.²⁵ The IR spectra of the acetate complexes **VI**–**VIII** display two bands assigned to the bidentate coordination of the acetate group ($\Delta\nu = \nu_{\text{asym}} - \nu_{\text{sym}}$, which were in the $73\text{--}122\text{ cm}^{-1}$ range).²⁶

All of these IR data confirm a bidentate ligand coordination for complexes **III**–**V** and a monodentate one for the others.

Electronic and EPR spectra

In order to obtain information concerning the stereochemistry of the metal ions, the UV–Vis spectra of the ligand and complexes were recorded in the solid phase. The electronic spectral data and the magnetic moments for the ligand and its complexes are given in Table III.

TABLE III. Electronic spectral data and magnetic moments for the ligand and its complexes

Compound	Observed bands cm^{-1} / nm	Assignments	μ_{eff} μ_B	Symmetry
Ligand (L)	37313 / 268 24752 / 404	$\pi \rightarrow \pi^*$ $n \rightarrow \pi^*$	—	—
[CuL ₂ (H ₂ O) ₂](NO ₃) ₂ ·2H ₂ O (I)	26316 / 380 14925 / 670	$n \rightarrow \pi$ ² E → ² T	2.14	Td
[NiL ₂ (H ₂ O) ₂](NO ₃) ₂ ·4H ₂ O (II)	39062 / 256 25252 / 396 17241 / 580 (ν_3) 9950 / 1005 (ν_1)	$\pi \rightarrow \pi^*$ $n \rightarrow \pi^*$ ³ T ₁ → ³ T ₁ (P) ³ T ₁ → ³ T ₂	4.45	Td
[CuL ₂ (H ₂ O) ₂](ClO ₄) ₂ (III)	19608 / 510 14204 / 704 ($\nu_1 + \nu_2$) 11223 / 891 (ν_3)	TS $d_{xz}, d_{yz} \rightarrow d_{x^2-y^2}$ $d_{xy} \rightarrow d_{x^2-y^2}$ $d_z^2 \rightarrow d_{x-y}$	1.77	Distorted Oh (D _{4h})
[CoL ₂ (H ₂ O) ₂](ClO ₄) ₂ (IV)	41841 / 239 25445 / 393 20576 / 486 (ν_3) 8802 / 1136 (ν_1)	$\pi \rightarrow \pi^*$ $n \rightarrow \pi^*$ ⁴ T _{1g} → ⁴ T _{1g} (P) ⁴ T _{1g} → ⁴ T _{2g}	5.57	Oh



TABLE III. Continued

Compound	Observed bands cm ⁻¹ / nm	Assignments	μ_{eff} μ_{B}	Symmetry
[NiL ₂ (H ₂ O) ₂](ClO ₄) ₂ (V)	39682 / 252 25445 / 393 16129 / 620 (v ₂) 10438 / 958 (v ₁)	$\pi \rightarrow \pi^*$ n $\rightarrow \pi^*$ ³ A _{2g} \rightarrow ³ T _{1g} (F) ³ A _{2g} \rightarrow ³ T _{2g}	3.05	Oh
[CuL ₂ (CH ₃ COO) ₂] (VI)	24096 / 415 12820 / 780	TS ² E _g \rightarrow ² T _{2g}	2.27	Oh
[CoL ₂ (CH ₃ COO) ₂] · 2H ₂ O (VII)	25125 / 398 18182 / 550 (v ₃) 9901 / 1010 (v ₁)	n $\rightarrow \pi^*$ ⁴ T _{1g} \rightarrow ⁴ T _{1g} (P) ⁴ T _{1g} \rightarrow ⁴ T _{2g}	5.26	Oh
[NiL ₂ (CH ₃ COO) ₂] (VIII)	39682 / 252 25252 / 396 15949 / 627 (v ₂) 10309 / 970 (v ₁)	$\pi \rightarrow \pi^*$ n $\rightarrow \pi^*$ ³ A _{2g} \rightarrow ³ T _{1g} (F) ³ A _{2g} \rightarrow ³ T _{2g}	3.34	Oh

The UV–Vis spectrum of the Schiff base ligand is characterized mainly by two absorption bands at 37313 (268 nm) and 24752 cm⁻¹ (404 nm), which may be assigned to $\pi \rightarrow \pi^*$ and n $\rightarrow \pi^*$ transitions. These transitions were also found in the spectra of the complexes, but they were shifted towards lower frequencies, confirming the coordination of the ligand to the metal ions.

The electronic spectrum of complex **I** showed a broad band at 14925 cm⁻¹, due to the ²E \rightarrow ²T transition, in a tetrahedral geometry around the cooper(II) ion. The electronic spectra of complex **III** showed absorption bands at 14204 and 11223 cm⁻¹, assignable to d_{xz}, d_{yz} \rightarrow d_{x²-y²} + d_{xy} \rightarrow d_{x²-y²} (v₁ + v₂) and d_{z²} \rightarrow d_{x²-y²} (v₃), respectively.²⁷ This is consistent for a D_{4h} geometry with a distorted octahedral environment around the cooper(II) ion. The absorption band at 19608 cm⁻¹ may be reasonably assigned to a charge transfer transition.

The electronic spectrum of complex **VI** showed a broad band at 12820 cm⁻¹, corresponding to a ²E_g \rightarrow ²T_{2g} transition in an octahedral stereochemistry around the cooper(II) ion. The observed magnetic moments 1.77 and 2.27 μ_{B} , for the complexes **III** and **VI**, respectively, usually correspond to an octahedral geometry.²⁸

The electronic spectra of the Co(II) complexes **IV** and **VII** of high-spin systems exhibited bands at 8802 and 20576 cm⁻¹ for complex **IV** and at 9901 and 18182 cm⁻¹ for complex **VII**, which may be assigned to v₁, ⁴T_{1g} \rightarrow ⁴T_{2g} and v₃, ⁴T_{1g} \rightarrow ⁴T_{1g}(P) transitions, respectively. The observed magnetic moment values of 5.57 and 5.26 μ_{B} for the Co(II) complexes suggest an octahedral geometry.²⁹

The electronic spectra of the Ni(II) complexes **V** and **VIII** also showed two bands at \approx 16000 and \approx 10400 cm⁻¹, assignable to ³A_{2g} \rightarrow ³T_{1g}(F) (v₂) and ³A_{2g} \rightarrow ³T_{2g} (v₁) transitions, respectively, in an octahedral geometry. The obser-



ved magnetic moment values 3.05 and 3.34 μ_B for the complexes **V** and **VIII** may be taken as additional evidence for their octahedral structure.²⁹

The complex **II** displayed two bands at 9950 and 17241 cm^{-1} , due to v_1 : $^3\text{T}_1 \rightarrow ^3\text{T}_2$ and v_3 : $^3\text{T}_1 \rightarrow ^3\text{T}_1(\text{P})$ transitions, respectively, and also, the magnetic moment value 4.45 μ_B indicates to a possible tetrahedral geometry.³⁰

The ligand field splitting energy ($10Dq$), interelectronic repulsion parameter (B) and nephelauxetic ratio (β) for the Co(II) and Ni(II) complexes were calculated using the secular equations given by König.^{31–33}

For the Ni(II) complexes **V** and **VIII**:

$$10Dq = v_1 \quad (1)$$

$$B = \frac{2v_1^2 + v_2^2 + 3v_1v_2}{15v_2 - 27v_1} \quad (2)$$

For the Ni(II) complex **II** and the Co(II) complexes **IV** and **VII**:

$$10Dq = 2v_1 - v_3 + 15B \quad (3)$$

$$B = \frac{1}{30} \sqrt{- (2v_1 - v_3) + (-v_1^2 + v_3^2 + v_1v_3)} \quad (4)$$

The values of the Racach parameter determined for the Ni(II) and Co(II) complexes are lower than usually observed for the free ions, 1041 and 971 cm^{-1} , respectively. The nephelauxetic ratio β depends on the ligand position on the nephelauxetic scale, indicating at the same time the degree of metal–ligand bond covalence.³⁴ For these complexes, the lower values suggest a larger degree of covalence.

The values of the electronic parameters, the ligand field splitting energy, the Racach interelectronic repulsion parameter and the nephelauxetic ratio are summarized in Table IV.

TABLE IV. Electronic parameters of the Co(II) and Ni(II) complexes

Compound	$10Dq / \text{cm}^{-1}$	B / cm^{-1}	β
[NiL ₂ (H ₂ O) ₂](NO ₃) ₂ ·4H ₂ O (I)	10944	552	0.53
[NiL ₂ (H ₂ O) ₂](ClO ₄) ₂ (V)	10438	677	0.65
[NiL ₂ (CH ₃ COO) ₂] (VIII)	10309	673	0.65
[CoL ₂ (H ₂ O) ₂](ClO ₄) ₂ (IV)	9992	864	0.89
[CoL ₂ (CH ₃ COO) ₂]·2H ₂ O (VII)	10966	623	0.64

The room temperature EPR spectra of the Cu(II) complexes **I**, **III** and **VI** were recorded in solid state. From the EPR spectrum of complex **I** the exact geometry of the metal ion cannot be proposed. The “g” parameters have only one value ($g_{\text{isotropic}} = 2.14$). The electronic spectra, the moment magnetic value and the relative isotropy of the “g” parameters indicate to the tetrahedral geometry of complex **I**.

An analysis of the EPR spectrum of complex **III** gave $g_{\parallel} = 2.15$ and $g_{\perp} = 2.07$. The trend $g_{\parallel} > g_{\perp}$,³⁵ which was observed for this complex, indicates a distorted octahedral geometry.

The EPR spectrum of complex **VI** displayed an isotropic signal with $g_i = 2.12$. The spectral data, magnetic susceptibility and isotropic value of the “ g ” factor suggest an octahedral geometry for this complex.

Thermal analysis

Thermal analysis by the TG and DSC techniques has proved to be very useful in determining the crystal water content in complexes and their thermal stability and decomposition mode under a controlled heating rate. Due to the explosive nature of perchlorate complexes, the thermal properties of only the nitrate and acetate complexes were investigated.^{36,37}

The determined temperature ranges and the corresponding percent mass losses are given in Table V.

The DSC curves of the Schiff base ligand (Fig. 2) showed a melting process located at 545.16 K (peak temperature) with $\Delta H = 118.5 \text{ J g}^{-1}$ (evaluated as the area of the endothermal DSC peak). The melting process is followed by exothermal decomposition with maximum at $T_{\max} = 600.16 \text{ K}$. The evaluation of the exothermal peak area gives a value of $\Delta H = -465.4 \text{ J g}^{-1}$.

The thermal behavior of the complexes depended on the nature and the environment around the metal ion. The TG/DTG and DSC curves of $[\text{CuL}_2(\text{H}_2\text{O})_2](\text{NO}_3)_2 \cdot 2\text{H}_2\text{O}$ complex are represented in Fig. 3. The decomposition of Cu(II) complex occurred in three stages.

The TG/DTG curves of $[\text{CuL}_2(\text{H}_2\text{O})_2](\text{NO}_3)_2 \cdot 2\text{H}_2\text{O}$ complex (**I**) showed a mass loss between 303.16 and 391.16 K due to dehydration with a loss of two lattice water molecules (exp. 3.65, calcd. 3.96 %). The second stage, from 391.16 to 429.16 K, corresponded to the elimination of two molecules of HNO_3 ,^{38,39} accompanied by the removal of two coordinated water molecules. The processes of elimination of molecules are indicated by the exothermal peak at 422.7 K on the DSC curve with $\Delta H = -951.22 \text{ J g}^{-1}$. The final stage, which occurred in the 429.16–1259.16 K temperature range, appeared as a complex process with more than one exothermal peak. The overall mass loss was observed to be 54.38 %. On DSC curve, the violent decomposition showed a strong exothermal effect with two overlapping peaks with a heat of decomposition (calculated as the peak area neglecting the partial superposition) of $\Delta H = -4670.22 \text{ J g}^{-1}$. This exothermal process is followed by another one with a maximum at 600.74 K and $\Delta H = -948.57 \text{ J g}^{-1}$. The final residue, estimated as CuO and carbon^{39,40}, was 23.7 %.

The TG/DTG and DSC curves of the $[\text{NiL}_2(\text{H}_2\text{O})_2](\text{NO}_3)_2 \cdot 4\text{H}_2\text{O}$ complex are represented in Fig. 4.

TABLE V. Thermoanalytical results for the M(II) complexes

Compound	TG range, K	Mass loss (found (calcd.), %)	Assignments
$[\text{CuL}_2(\text{H}_2\text{O})_2](\text{NO}_3)_2 \cdot 2\text{H}_2\text{O}$	303.16–391.16	3.65 (3.96)	Loss of 2 lattice water molecules
	391.16–429.16	18.29 (17.80)	Loss of 2 coordinated water molecules + 2HNO_3
	429.16–1259.16	54.38	Removal of the ligand
	>1259.16	23.68	$\text{CuO} + \text{C}$
$[\text{NiL}_2(\text{H}_2\text{O})_2](\text{NO}_3)_2 \cdot 4\text{H}_2\text{O}$	303.16–393.16	7.47 (7.64)	Loss of 4 lattice water molecules
	393.16–537.16	26.40 (25.60)	Loss of 2 coordinated water molecules + $2\text{HNO}_3 +$ removal of one Py molecule
	537.16–1123.16	39.51	Removal of the ligand
	>1123.16	26.62	$\text{NiO} + \text{C}$
$\text{Cu}(\text{L})_2(\text{CH}_3\text{COO})_2$	478.16–523.16	19.45 (19.00)	Removal of two Py molecules
	523.16–634.16	66.01 (66.15)	Removal of the ligand
	634.16–713.16	5.11 (5.29)	Loss of CO_2 molecule
	>713.16	9.42 (9.56)	CuO
$[\text{CoL}_2(\text{CH}_3\text{COO})_2] \cdot 2\text{H}_2\text{O}$	388.16–458.16	3.88 (4.17)	Loss of 2 lattice water molecules
	505.16–563.16	18.72 (18.31)	Removal of two Py molecules
	563.16–663.16	64.24 (63.13)	Removal of the ligand
	663.16–718.16	4.88 (5.10)	Loss of CO_2 molecule
$\text{Ni}(\text{L})_2(\text{CH}_3\text{COO})_2$	>445	9.04 (9.29)	Co_3O_4
	538.16–603.16	19.18 (19.12)	Removal of two Py molecules
	603.16–733.16	66.42 (66.54)	Removal of the ligand
	733.16–773.16	5.46 (5.32)	Loss of CO_2 molecule
	>773.16	8.94 (9.02)	NiO

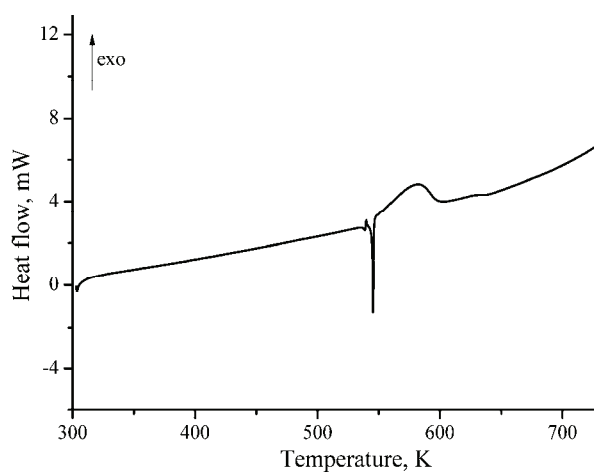


Fig. 2. DSC curve of the ligand.

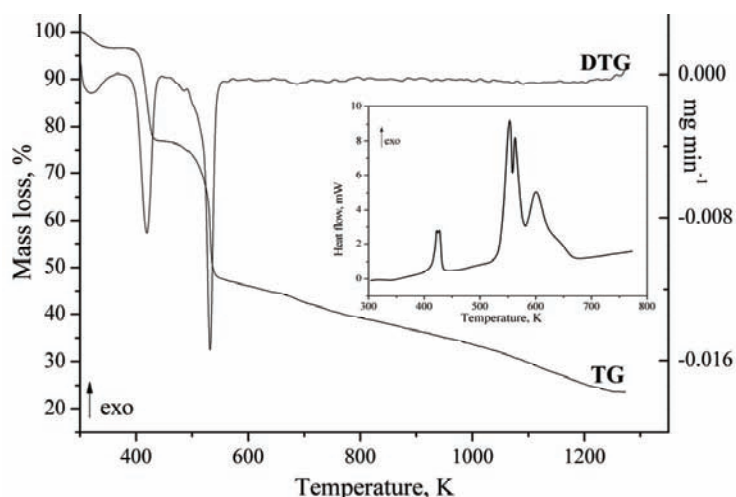


Fig. 3. TG, DTG and DSC (inset) curves of $[\text{CuL}_2(\text{H}_2\text{O})_2](\text{NO}_3)_2 \cdot 2\text{H}_2\text{O}$ (I).

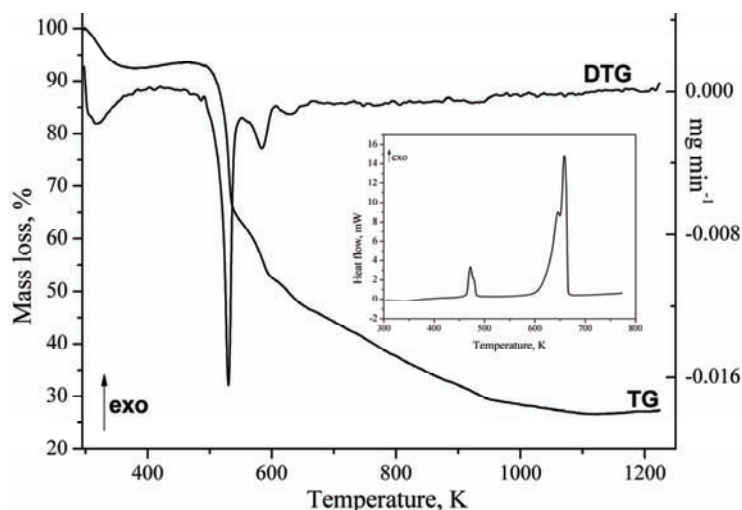


Fig. 4. TG, DTG and DSC (inset) curves of $[\text{NiL}_2(\text{H}_2\text{O})_2](\text{NO}_3)_2 \cdot 4\text{H}_2\text{O}$ (II).

The $[\text{NiL}_2(\text{H}_2\text{O})_2](\text{NO}_3)_2 \cdot 4\text{H}_2\text{O}$ complex showed almost the same three-stage decomposition process. The first stage occurred in the temperature range 303.16–393.16 K, with a mass loss of 7.47 % due to the removal of four lattice water molecules (calcd. 7.64 %). The second step, between 393.16 and 537.16 K, was complex and was also due to the loss of two coordinated water molecules together with the loss of two molecules of HNO_3 and one molecule of pyridine. The decomposition process is indicated by the DSC peak at 471.18 K, with $\Delta H = -641.11 \text{ J g}^{-1}$. The third stage (from 537.16–1123.16 K) was due to the total

decomposition of the ligand. The observed mass loss was 39.51 %. This step was accompanied by an exothermal process at 658.69 K on the DSC curve, with $\Delta H = -7028.00 \text{ J g}^{-1}$. The residue at 1123.16 K amounted to 26.62 % and corresponded to nickel oxide and carbon.^{39,40}

The absence of any mass loss under 473.16 K indicates that the Cu(II) and Ni(II) acetate complexes contained neither coordinated water molecules nor water of crystallization. Their thermal decompositions revealed them to be anhydrous, which is consistent with the elemental and spectral data.

The thermal decomposition of $\text{Cu}(\text{L})_2(\text{CH}_3\text{COO})_2$ proceeded in three stages. The TG, DTG and DSC curves are given in Fig. 5. The complex was stable up to 478.16 K. The first step of thermal decomposition occurred in the range 478.16–523.16 K and corresponds to the removal of two pyridine molecules (exp. 19.45, calcd. 19.00 %). The second (from 523.16–643.16 K) and third (from 643.16–713.16 K) stages may be due to the removal of the remaining part of the ligand and the acetate group.⁴¹ The observed mass losses in these temperature ranges were 66.01 (calcd. 66.15 %) and 5.11 % (calcd. 5.92 %), respectively. On the DSC curve, the decomposition process is complex with at least three exothermal peaks with $\Delta H = -8234.40 \text{ J g}^{-1}$ (obtained as the peak area in the 523.16–643.16 K temperature range, neglecting the partial superposition). The residue, estimated as copper oxide, had a mass of 9.42 %, compared with the calculated value of 9.56 %.

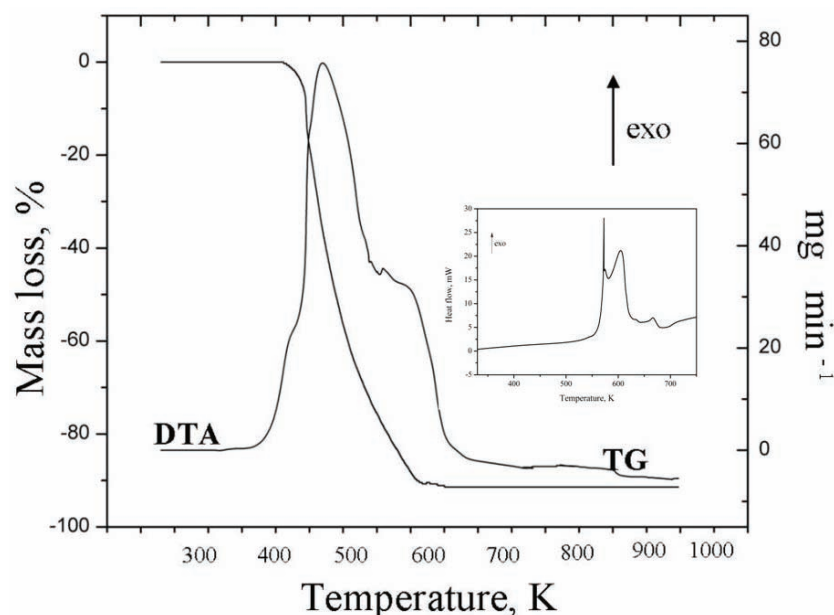


Fig. 5. TG, DTG and DSC (inset) curves of $\text{Cu}(\text{L})_2(\text{CH}_3\text{COO})_2$ (**VI**).

The TG, DTG and DSC curves of $[\text{CoL}_2(\text{CH}_3\text{COO})_2]\cdot 2\text{H}_2\text{O}$ are shown in Fig. 6. The thermal decomposition of the Co(II) acetate complex proceeded in four stages. The thermal dehydration of this complex occurred between 388.16 and 458.16 K, with a mass loss of 3.88 % (calcd. 4.17 %). Two moles of lattice water molecules were removed in this dehydration stage. The process was accompanied by an endothermal effect at 425.78 K on the DSC curve, with $\Delta H = -163.59 \text{ J g}^{-1}$. The elimination of crystal water molecules at $\approx 426 \text{ K}$ suggests that these are strongly bound in the crystal lattice of the complex.³⁹ The second (from 505.16–563.16 K) and third (from 563.16–663.16 K) stages may be due to the decomposition of ligand with an observed mass losses of 18.72 (calcd. 18.31 %) and 64.24 % (calcd. 63.13 %), respectively. These steps were accompanied by a complex decomposition process with three consecutive and overlapping exothermal peaks on the DSC curve, with $\Delta H = -1303.68 \text{ J g}^{-1}$ (obtained as the peak area in the 453.16–603.16 K temperature range, neglecting the partial superposition). The fourth stage occurred in the 663.16–718.16 K temperature range, corresponding to the loss of the acetate group, with a mass loss of 4.88 % (calcd. 5.10 %). The process is indicated by the DSC peak with maximum at 718.16 K. The heat of decomposition had a value of $\Delta H = -314.35 \text{ J g}^{-1}$. The final residue, estimated as Co_3O_4 ,^{42,43} had a mass of 9.04 %, compared to the calculated value of 9.29 %.

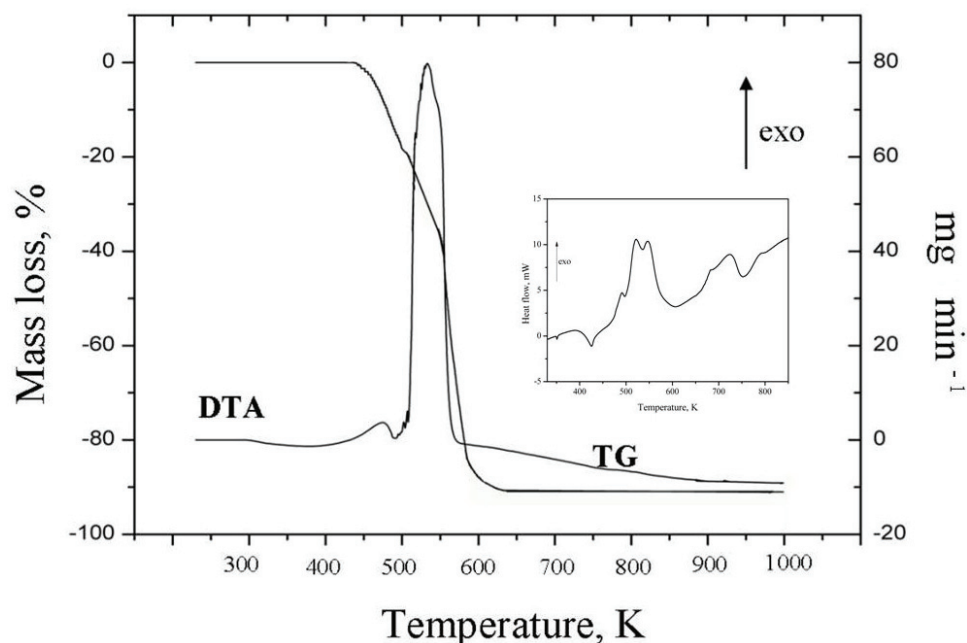


Fig. 6. TG, DTG and DSC (inset) curves of $[\text{CoL}_2(\text{CH}_3\text{COO})_2]\cdot 2\text{H}_2\text{O}$ (VII).

As predicted, the Ni(II) acetate complex was stable up to 538.16 K. The TG, DTG and DSC curves are shown in Fig. 7. According to the TG analysis, the thermal decomposition of this complex was a three-stage process. The first mass loss occurred between 538.16 and 603.16 K, with two exothermal peaks on the DSC curve at 545.16 K, with $\Delta H = -241.13 \text{ J g}^{-1}$ and 582.46 K, with $\Delta H = -92.15 \text{ J g}^{-1}$, and is attributed to the removal of two molecules of pyridine (exp. 19.18, calcd. 19.12 %). The removal of the remaining part of the ligand followed in the second stage, between 603.16 and 733.16 K, with a mass loss of 66.42 % (calcd. 66.54 %). The process was indicated by the DSC peak at 698.03 K, with $\Delta H = -3174.03 \text{ J g}^{-1}$. The third stage between 733.16–773.16 K with a DSC peak at 790.76 K and $\Delta H = -2689.41 \text{ J g}^{-1}$ corresponds to the loss of the acetate group. The observed mass loss was 5.46 %, which is consistent with the theoretical value of 5.32 %. The residue, estimated as NiO, had a mass of 8.94 %, compared with the calculated value of 9.02 %.

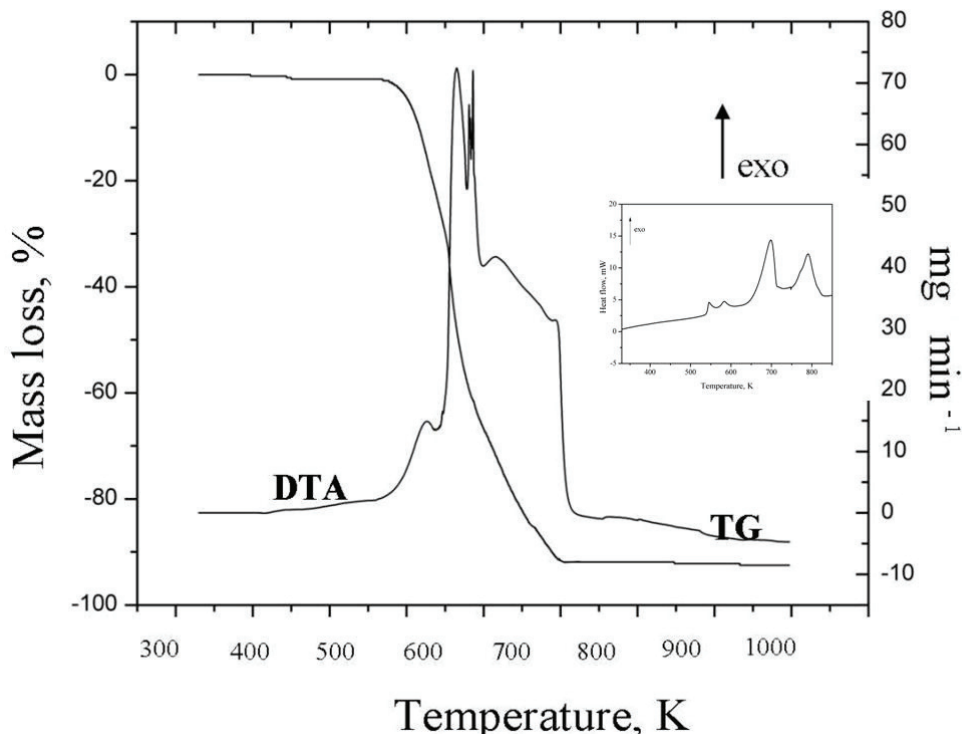
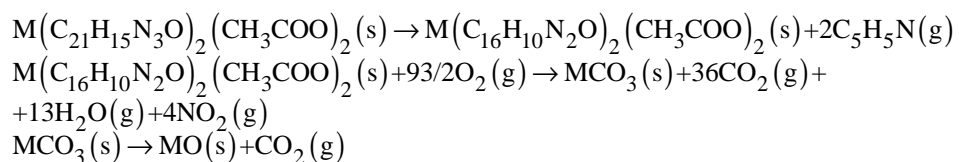


Fig. 7. TG, DTA and DSC (inset) curves of $\text{Ni}(\text{L})_2(\text{CH}_3\text{COO})_2$ (**VIII**).

From the thermal investigation of the Cu(II) and Ni(II) acetate complexes, it can be concluded that the decomposition proceeds in the following three stages:



where M is Cu(II) or Ni(II).

Based on the above analytical, spectral and magnetic data together with the thermal decomposition studies, the structural formula and the stoichiometry, given in Fig. 8, are proposed.

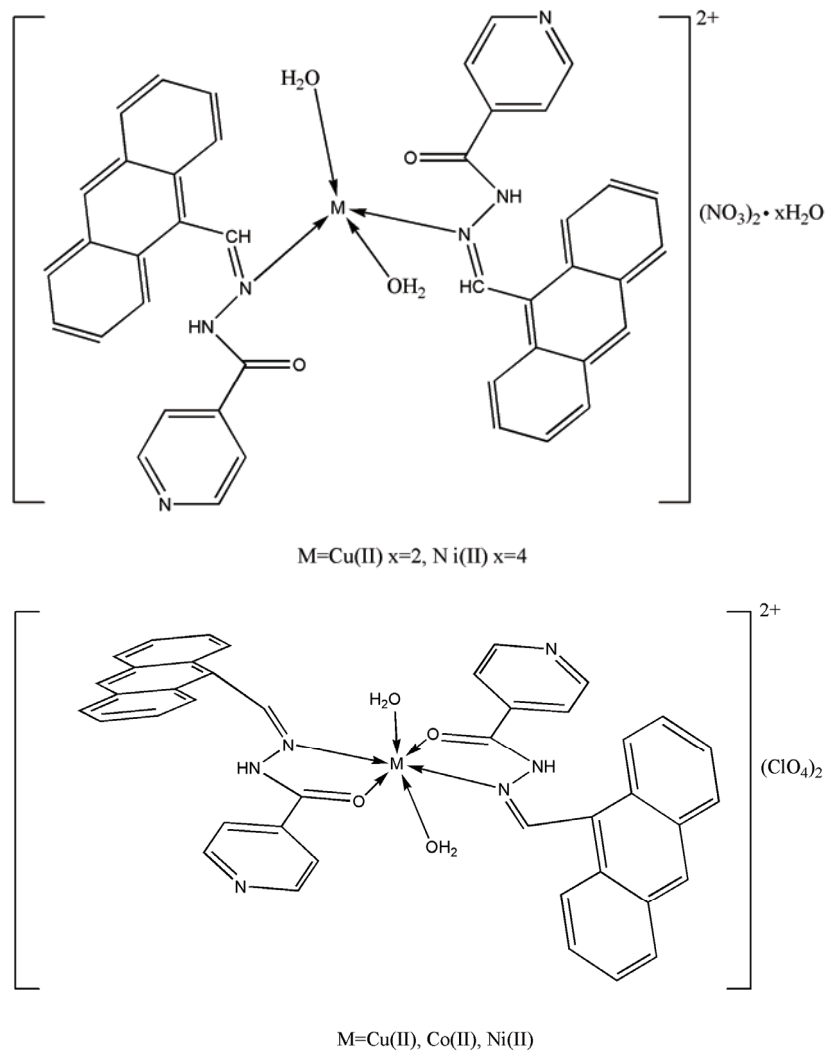
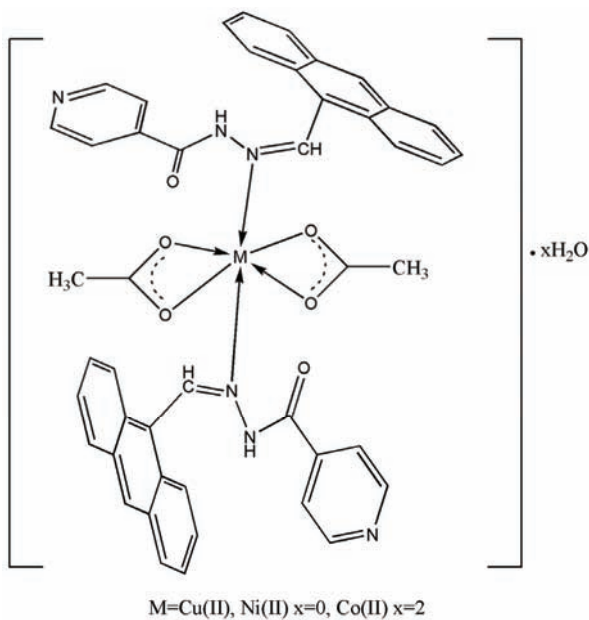


Fig. 8. Structural formula of the $ML_2X_2 \cdot xH_2O$ complexes.

Fig. 8 (continued). Structural formula of the $\text{ML}_2\text{X}_2\cdot\text{xH}_2\text{O}$ complexes.

CONCLUSIONS

Eight new complexes of Cu(II), Co(II) and Ni(II) with isonicotinic acid 2-(9-anthrylmethylene)-hydrazide were synthesized and characterized by analytical, spectral and thermal studies. The spectral studies indicated that hydrazone act as a neutral monodentate ligand coordinating through the nitrogen of the azomethine group or as a bidentate ligand using both the azomethine nitrogen and the amide oxygen. The nitrate complexes have a tetrahedral geometry and the others an octahedral one around the metal ion. The thermal decomposition of the hydrated **I**, **II** and **VII** complexes began with the release of crystallization water in the first stage. During heating, the nitrate complexes lost two coordinated water molecules in the second stage. The anhydrous acetate complexes of Cu(II) and Ni(II) were the most stable. Their decomposition commenced above 473.16 K. The thermal data are in agreement with the spectral and elemental data.

ИЗВОД

КОМПЛЕКСИ ПРЕЛАЗНИХ МЕТАЛА(II) СА 2-(9-АНТРИЛМЕТИЛЕН)ХИДРАЗИДОМ
ИЗОНИКОТИНСКЕ КИСЕЛИНЕMARIANA LOREDANA DIANU¹, ANGELA KRIZA¹, NICOLAE STANICA² и ADINA MAGDALENA MUSUC²¹*University of Bucharest, Faculty of Chemistry, Department of Inorganic Chemistry, 23 Dumbrava Rosie St., 020464 Bucharest* и ²*Romanian Academy, „Ilie Murgulescu“ Institute of Physical Chemistry, 202 Spl. Independentei, P.O. Box 12–194, 060021 Bucharest, Romania*

Синтетизовани су и охарактерисани нови комплекси Cu(II), Co(II) и Ni(II) са 2-(9-антрилметилен)хидразидом изоникотинске киселине. За карактеризацију комплекса употребљене су различите аналитичке и физичкохемијске методе, као што су елементална и термална анализа, магнетна и кондуктометријска мерења, електронски, ESR и IR спектри. Инфрацрвена спектроскопска испитивања су показала да су у испитиваним комплексима одговарајући лиганди типа Шифових база монодентатно, или бидентатно координовани, као и да пиридински атом азота код ових лиганада не учествује у координацији. Одговарајућим нитратним комплексима приписана је тетраедарска, док је за остале испитиване комплексе претпостављена октаедарска геометрија. Добивени резултати термалних испитивања су у складу са претпостављеним формулама испитиваних комплекса.

(Примљено 23. новембра 2009, ревидирано 6. априла 2010)

REFERENCES

1. S. Rollas, S. G. Küçükgüzel, *Molecules* **12** (2007) 1910
2. E. W. Ainscough, A. M. Brodie, W. A. Denny, G. J. Finlay, S. A. Gothe, J. D. Ranford, *J. Inorg. Biochem.* **77** (1999) 125
3. B. Bottari, R. Maccari, F. Monforte, F. Ottana, E. Rotondo, M. G. Vigorita, *Bioorg. Med. Chem. Lett.* **10** (2000) 657
4. S. K. Sridhar, M. Saravanan, A. Ramesh, *Eur. J. Med. Chem.* **36** (2001) 615
5. K. B. Koçyiğit, S. Rollas, *Farmaco* **57** (2002) 595
6. R. K. Agarwal, D. Sharma, L. Singh, H. Agarwal, *Bioinorg. Chem. Appl.* **2006** (2006) 1
7. N. K. Singh, N. Singh, A. Sodhi, A. Shrivastava, *Transition Met. Chem.* **21** (1996) 556
8. N. K. Singh, N. Singh, G. C. Prasad, A. Sodhi, A. Shrivastava, *Bioorg. Med. Chem.* **5** (1997) 245
9. B. V. Agarwala, S. Hingorani, G. A. Nagna Gowda, *Inorg. Chim. Acta* **176** (1990) 149
10. R. C. Maurya, R. Verma, T. Singh, *Synth. React. Inorg. Met.-Org. Chem.* **33** (2003) 309
11. M. Donia, H. A. El-Boraey, M. F. El-Samalehy, *J. Therm. Anal. Calorim.* **73** (2003) 987
12. M. Amirnasr, R. Houriet, S. Meghdadi, *J. Therm. Anal. Calorim.* **67** (2002) 523
13. M. Sekerci, F. Yakuphanoglu, *J. Therm. Anal. Calorim.* **75** (2004) 189
14. H. A. El-Boraey, *J. Therm. Anal. Calorim.* **81** (2005) 339
15. S. A. AbouEl-Enein, *J. Therm. Anal. Calorim.* **91** (2008) 929
16. C. K. Modi, B. T. Thaker, *J. Therm. Anal. Calorim.* **94** (2008) 567
17. L. Mitu, N. Raman, A. Kriza, N. Stanica, M. Dianu, *Asian J. Chem.* **21** (2009) 5749
18. L. Mitu, N. Raman, A. Kriza, N. Stanica, M. Dianu, *J. Serb. Chem. Soc.* **74** (2009) 1075
19. G. Macarovici, *Inorganic Quantitative Chemical Analysis*, Ed. Academiei, Bucharest, 1979
20. W. J. Geary, *Coord. Chem. Rev.* **7** (1971) 81
21. K. Nakamoto, *Infrared and Raman Spectra of Inorganic and Coordination Compounds*, Wiley, New York, 1986



22. R. S. Baligar, V. K. Revankar, *J. Serb. Chem. Soc.* **71** (2006) 1301
23. A. Z. El-Sonbati, *Transition Met. Chem.* **16** (1991) 45
24. K. B. Yatsimirskii, *Pure Appl. Chem.* **49** (1977) 115
25. S. D. Ross, *Spectrochim. Acta* **18** (1962) 225
26. U. Casellato, P. A. Vigato, N. Vidali, *Coord. Chem. Rev.* **26** (1978) 85
27. B. P. Lever, *Inorganic Electronic Spectroscopy*, 2nd ed., Elsevier Science, New York, 1984
28. R. L. Carlin, *Magnetochemistry*, Springer, Berlin Heidelberg, 1986
29. F. A. Cotton, G. Wilkinson, *Advanced Inorganic Chemistry*, Wiley Interscience, New York, 1976
30. C. I. Lepadatu, M. Andruh, *Forma moleculelor anorganice. O introducere in stereochemia anorganica*, Ed. Academiei Romane, Bucharest, 1998 (in Romanian)
31. E. König, S. Kremer, *Ber. Bunsenges Phys. Chem.* **78** (1974) 786
32. E. König, R. Schnakig, *Phys. Status Solidi* **B77** (1976) 657
33. E. König, *Struct. Bond.* **9** (1971) 175
34. D. Marinescu, *Chimie Coordinativa – Principii generale*, Ed. Universitatii, Bucharest, 1995 (in Romanian)
35. S. Chandra, X. Sangeetika, *Spectrochim. Acta A* **60** (2004) 147
36. C. Wei, W. J. Rogers, M. S. Mannan, *J. Therm. Anal. Calorim.* **83** (2006) 125
37. G. Sing, D. K. Pande, *J. Therm. Anal. Calorim.* **82** (2005) 353
38. Z. H. A. El-Wanab, M. M. Mashaly, A. A. Salma, B. A. El-Shetary, A. A. Faheim, *Spectrochim. Acta A* **60** (2004) 2861
39. M. Lalia-Kantouri, L. Tzavellas, D. Paschalidis, *J. Therm. Anal. Calorim.* **91** (2008) 937
40. S. U. Din, M. Umar, *J. Therm. Anal. Calorim.* **58** (1999) 61
41. G. G. Mohamed, Z. H. A. El-Wahab, *J. Therm. Anal. Calorim.* **73** (2003) 347
42. D. Czakis-Sulikowska, J. Radwańska-Doczekalska, M. Markiewicz, M. Pietrzak, *J. Therm. Anal. Calorim.* **93** (2008) 789
43. G. Bannach, A. B. Siqueira, E. Y. Ionashiro, E. C. Rodrigues, M. Ionashiro, *J. Therm. Anal. Calorim.* **90** (2007) 873.